Sensors & Diagnostics

PAPER

View Article Online
View Journal | View Issue

Cite this: *Sens. Diagn.*, 2025, **4**, 767

CO_2-sensitive inks for the rapid measurement of total viable count (TVC) using micro-respirometry†

Sean Cross, Christopher O'Rourke and Andrew Mills *

At present, micro-respirometry for measuring total viable count, O_2 μR-TVC, is based on the time taken, TT, for an inoculum to significantly reduce the dissolved O_2 level (typically from 21% to ≤ 10.5%). Here, a simple kinetic model relevant to μR-TVC is presented which describes the growth of the bacteria from an initial inoculum, N_o, to a maximum level, N_{max}, and concomitant consumption of O_2 and generation of CO_2, in which the half-way time point, $t^*_{1/2}$, corresponds to N_{max}/N_o = 0.5, at which point $\%O_2$ = $\%CO_2$ = 10.5%. The model shows that it is not possible to reduce the TT in O_2 μR-TVC below $t^*_{1/2}$, as TT increases above $t^*_{1/2}$ with increasing sensitivity of the O_2 sensor. In contrast, the same model shows that if a CO_2 sensor is used instead, TT can be reduced significantly below $t^*_{1/2}$ and consequently CO_2 μR-TVC could be made much faster than conventional O_2 μR-TVC. To test this model prediction, a range of colourimetric CO_2 sensors of varying sensitivity, α, were prepared and used to make CO_2 μR-TVC measurements. The results confirm that the greater the sensitivity of the sensor, the shorter the TT, as predicted by the kinetic model. Two CO_2 indicators, one of moderate sensitivity and one of high sensitivity were used to generate straight-line log(CFU mL^{-1}) *vs.* TT calibration plots, which can then be used to determine the unknown TVCs of subsequent samples. The future of CO_2 μR-TVC as a possible new, faster alternative to conventional O_2 μR-TVC is discussed briefly.

Received 27th May 2025,
Accepted 30th June 2025

DOI: 10.1039/d5sd00078e

rsc.li/sensors

1. Introduction

The measurement of the total viable count of aerobes, TVC, (units: colony forming units, CFU mL^{-1}) is a core feature of microbiological research and plays a key health and safety role in many sectors, including in the food and drinks industries, as well as in healthcare and environmental monitoring.[1] TVC is usually measured using the aerobic plate counting method, APC, which is laborious, time consuming and slow, typically requiring up to 72 h to produce results.[2,3] Consequently, there is considerable interest in developing faster, more cost-effective alternatives that, unlike APC, are amenable to automation. One such alternative is micro-respirometry, μR.[4]

In μR for measuring TVC, *i.e.*, O_2 μR-TVC, the level of dissolved O_2 is monitored as a function of incubation time, *t*. The measurement of O_2 is usually carried out using an O_2 sensor which employs a phosphorescent dye, D, the excited-state lifetime of which is quenched by molecular oxygen. The relationship between the measured excited-state lifetime, τ, and the ambient oxygen concentration, $\%O_2$, is described by the Stern–Volmer equation,

$$\tau/\tau_o = 1 + K_{sv}\%O_2 \quad (1)$$

where τ and τ_o are the lifetimes of D in the presence and absence of O_2, respectively and, K_{sv}, the Stern–Volmer constant, is equal to the product, $\tau_o \cdot k_q$, where k_q is the rate constant associated with the quenching of the excited state of the dye by O_2. Usually, k_q depends primarily on the permeability of O_2 in the polymer which encapsulates the dye, whereas τ_o is an intrinsic property of the dye itself.

Typically, the dye used in O_2 μR-TVC is a Pt porphyrin, such as Pt(II) tetraphenyl tetrabenzoporphyrin (PtBP), encapsulated in a polymer such as polyvinyl butyral (PVB), and has a luminescent lifetime of *ca.* 50 and 21 μs in the absence and presence of air, respectively, giving the sensor a K_{sv} value of 0.071% O_2^{-1}.[5] In O_2 μR-TVC, τ is monitored as a function of incubation time, and the threshold time, TT, is recorded when the value of τ reaches its midpoint, *i.e.*, when $\tau = (\tau_o + \tau_{air})/2$, as the bacteria respire and deplete dissolved O_2 in the growth medium. In O_2 μR-TVC, it is found that

School of Chemistry and Chemical Engineering, Queens University Belfast, Stranmillis Road, Belfast, BT9 5AG, UK. E-mail: andrewmills@qub.ac.uk

† Electronic supplementary information (ESI) available. See DOI: https://doi.org/10.1039/d5sd00078e

log(TVC) of the bacterium under test is proportional to TT, and this feature is used to construct a log(TVC) *vs.* TT calibration graph which can then be used to determine the TVC of any subsequent test sample used to inoculate the growth medium, *via* its measured value of TT.[5] Note that in O_2 μR-TVC, eqn (1) is not usually used to calculate the $\%O_2$, instead it is sufficient to use the midpoint lifetime value, $\tau = (\tau_o + \tau_{air})/2$, to identify the value of TT.

When compared to the traditional APC method for measuring TVC, O_2 μR-TVC is relatively rapid (usually < 12 h). Additionally, unlike APC, it is amenable to automation and thus commercial TVC-measuring systems based on O_2 μR-TVC have been developed.[6] However, although relatively fast, the speed of measurement in O_2 μR-TVC is limited by the fact that TT corresponds to the time taken for the dissolved O_2 concentration to drop significantly, from its initial value of 21% (as the initial inoculum/growth medium is air saturated) to typically ≤10.5%. This marked drop in $\%O_2$ only occurs when the bacterial load in the growth medium has increased substantially, typically to $\geq 5 \times 10^7$ CFU mL^{-1}. It follows that for any aerobe used in O_2 μR-TVC, the measured value of TT associated with any inoculum (like 10^4 CFU mL^{-1}) is limited by the bacterium's growth kinetics and so cannot be reduced significantly by increasing the sensitivity of the O_2 sensor.[5]

The above feature can be simply demonstrated using a kinetic model based on the often-cited continuous logistic equation for bacterial growth kinetics,[7] which assumes that the rate of growth, $dN(t)/dt$, at any time, t, is proportional to both the size of the population, $N(t)$, and the remaining material resources in the growth medium. The integrated form of the continuous logistic rate equation is,

$$N(t) = N_{max}/[1 + A^*\exp(-kt)] \quad (2)$$

where N_{max} is the maximum number of bacteria the growth medium can finally support, $A^* = (N_{max}/N_o - 1)$, k is a proportionality constant, and N_o is the population of the bacteria at $t = 0$.[7] If we assume, for simplicity, that in O_2 μR-TVC the observed variation in the $\%O_2$ dissolved in the growth medium with incubation time has a profile which mirrors that of the $N(t)$ *vs.* t bacteria growth profile described by eqn (2), then it is possible to derive the following simple expression for the observed variation in $\%O_2$ with respect to the unitless time parameter, t^*,

$$\%O_2 = 21(1 - 1/[1 + A^*\exp(-t^*)]) \quad (3)$$

where t^* is $= kt$ and assuming that at $t = 0$, $\%O_2 = 21\%$. Mirror image plots of the variation in $N(t)$ and $\%O_2$ *vs.* t^*, calculated using the kinetic model eqn (2) and (3), respectively, are illustrated in Fig. S1 in the ESI† file, based on N_o and N_{max} values of 10^4 and 10^8 CFU mL^{-1}.

Using the kinetic model, it can be shown that in O_2 μR-TVC, when the lifetime, τ, of the O_2 sensor reaches its half-way value, $(\tau_o + \tau_{air})/2$, at the associated threshold time, t^*_{TT}, the corresponding $\%O_2$ is given by the following expression,

$$\%O_2(TT) = 21/(2 + 21K_{sv}) \quad (4)$$

Consequently, eqn (3) and (4) of the above kinetic model can be used to illustrate the effect of changing the sensitivity, K_{sv}, of the O_2 sensor on t^*_{TT}, the TT measured in O_2 μR-TVC. Reassuringly, the model also predicts that, for any O_2 sensor, *i.e.*, any K_{sv} value, the log of the initial inoculum, $\log(N_o)$, is directly proportional to t^*_{TT}, as is found in practice in O_2 μR-TVC; see Fig. S2 and S3 in the ESI.† Thus, the model shows that the classic calibration straight line plot of log(CFU mL^{-1}), *i.e.*, log(TVC), *vs.* TT, which underpins O_2 μR-TVC, is entirely consistent with the bacterial growth kinetics described by eqn (1).[7,8]

In a simple model calculation, it was assumed that N_o and N_{max} were 10^4 and 10^8 CFU mL^{-1}, respectively, and eqn (3) was used to calculate the variation of $\%O_2$ *vs.* t^* illustrated in Fig. 1. As expected, the profile shows that after the usual lag phase associated with bacterial growth, there is a rapid drop in the level of dissolved O_2 as the bacteria enter their exponential growth phase. The $\%O_2$ *vs.* t^* data in Fig. 1 and eqn (4) were then used to predict the variation in TT in O_2 μR-TVC, t^*_{TT}, for sensors with sensitivities (K_{sv}) ranging from 0.01 to 0.49% O_2^{-1}. This range corresponds to using O_2-sensitive dyes entrapped in the same polymeric medium, with τ_o values spanning the experimentally relevant range of 7 to 350 μs. The resulting plot of the K_{sv} *vs.* t^*_{TT} is illustrated in Fig. 1 by the broken red line.

The K_{sv} *vs.* t^*_{TT} plot illustrated in Fig. 1 (broken red line) shows that as the sensitivity of the O_2 sensor increases, the value of t^*_{TT} rises above a minimum value of $t^*_{1/2}$, at which $N_o/N_{max} = 0.5$ and $\%O_2 = 10.5\%$. This plot illustrates the general feature of O_2 μR-TVC, that for any given inoculum, the measured TT value is always greater than $t^*_{1/2}$ and increases with increasing O_2 sensor sensitivity.[5]

In contrast to the above, when the O_2 sensor is replaced with a CO_2 sensor, as in CO_2 μR-TVC, the same kinetic model predicts that TT values can fall below $t^*_{1/2}$. This suggests that, by employing highly sensitive CO_2 sensors, CO_2 μR-TVC could enable significantly faster TVC measurements than O_2 μR-TVC. It is worth noting that CO_2 μR-TVC is a relatively new technology, and most recent reviews of CO_2 sensors focus on their applications in food packaging.[9,10] In contrast, fluorescence-based O_2 sensors are very well established and widely used in fields such as environmental monitoring, biomedical science and food packaging, as highlighted in two recent reviews.[11,12] Consequently, unlike the emerging CO_2 μR-TVC approach, O_2 μR-TVC is a well-established technique that continues to attract academic research.[8,13]

The very short TT values predicted for CO_2 μR-TVC represent a significant advantage over its established, commercial O_2 μR-TVC counterpart, as it implies that, for the same bacterial sample under test, CO_2 μR-TVC has the

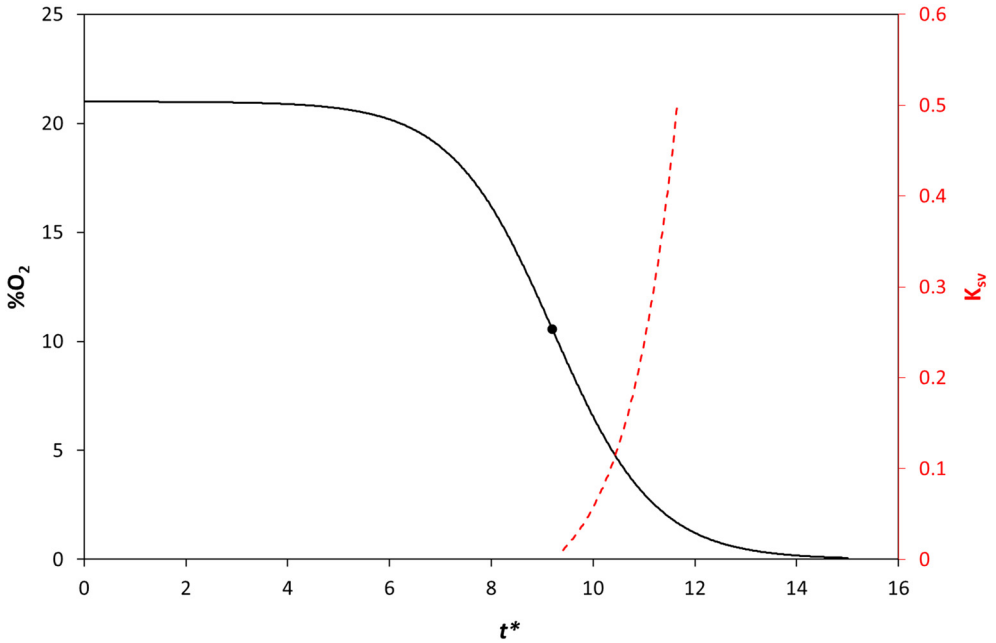

Fig. 1 Plot of $\%O_2$ *vs.* unitless time parameter t^*, calculated using eqn (3), assuming N_{max} and N_o are 10^8 and 10^4 CFU mL^{-1}, respectively. The broken red line is a plot of the variation in t^*_{TT} for a series of O_2 sensors with different K_{SV} values, calculated using eqn (3) and (4). The black point marks the t^* value (9.2), = $t^*_{1/2}$, when N_o/N_{max} = 0.5 and $\%O_2$ = 10.5%.

potential to measure TVC much more rapidly. O_2 μR-TVC is already attracting significant interest, as it has been shown to be much faster (typically 3–4×) than the gold-standard APC method that is currently employed by most laboratories to measure TVC. Like O_2 μR-TVC, and in contrast to APC, CO_2 μR-TVC can be readily automated, is inexpensive and does not require significant technical support nor a large amount of plasticware. As such, CO_2 μR-TVC has strong potential as a high throughput, ultra-rapid methodology for TVC determination. In this paper, a simple kinetic model is used to demonstrate that the TT in CO_2 μR-TVC can be reduced significantly by increasing the sensitivity (α) of the CO_2 sensor, and this prediction is validated using a range of easily fabricated CO_2 sensors spanning a wide range of sensitivities. The results indicate that CO_2 μR-TVC has the potential to become a leading technique for rapid TVC measurement.

2. Experimental

2.1. Materials

Elastosil® A07 silicone rubber was purchased from Wacker (Munich, Germany). Tyvek® envelopes (A4, 55 gsm, 0.143 mm thickness) (DuPont, Delaware, U.S.) were purchased from Amazon (Washington, U.S.). The 25 μm LDPE film used to heat-seal the CO_2 sensors was purchased from Goodfellow (Cambridge, UK). KWIK STIK stock cultures of *Escherichia coli* ATCC 8739 (*E. coli*) were obtained from Microbiologics (St Cloud, MN, USA). All the gases and gas mixtures used in this work (such as compressed air, CO_2, Ar, 0.1%, 1%, 2%, 5% and 25% CO_2 in air) were purchased from BOC (Surrey, UK) and were of the highest purity available. The water used to make up the aqueous solutions was high purity, doubly distilled and deionised. The Luria–Bertani broth (LB) growth medium was purchased from Sigma-Aldrich. Details regarding the preparation and bacterial load measurements, made using the plate counting method, and carried out in triplicate, are described elsewhere.[2,5,14,15]

2.2. Preparation of CO_2 sensors

Two different types of colourimetric CO_2 sensor were used in this study, namely ones in which the polymeric dye-encapsulating medium was either, (i) solvent-soluble silicone or (ii) water-soluble hydroxypropyl cellulose (HPC). A typical solvent-based sensor ink was prepared by dissolving 0.012 g of the pH indicator dye in 1 mL of a tetraoctylammonium hydroxide (TOAH) solution (20 wt% in MeOH). 3 g of Elastosil® A07 silicone rubber were then added to 1 mL of the above dye solution, along with 0.5 mL toluene. The final solution was stirred at room temperature overnight to ensure all the components were dissolved and then stored in a fridge. A typical water-based ink was prepared by dissolving 0.1 g of the dye in a solution comprising 2.5 mL of deionised water and 1 mL tetrabutylammonium hydroxide (TBAH) (40% in water). To 2 mL of this solution were added 10 g of a 10 wt% aqueous solution of HPC, 1.5 g glycerol and 1 mL of the TBAH solution, and the final solution stirred at room temperature for 1 h before being stored in a fridge. Other work showed that a thymol blue (TB) ink, in which the silicone polymer was replaced by ethyl cellulose, was particularly CO_2 sensitive, and so a sensor based on this

solvent-based ink, referred to henceforth as TB†, was also assessed as part of this study. The TB† sensor ink was prepared by dissolving 0.1 g of the dye in a solution comprising 1 mL of methanol and 1 mL TOAH solution (20 wt% in MeOH). 5 g ethyl cellulose (10% in toluene) were then added to 2 mL of the above dye solution, as well as 1 mL tributyl phosphate, and the final solution stirred at room temperature for 1 h before being stored in a fridge.[16]

Before use, each type of ink taken from the fridge was allowed to warm up to room temperature, 20 °C, (15 min) before being spread evenly on Tyvek (which provided a white, gas-permeable background support substrate) using a K-Bar No. 3 ink spreader.[17]

For each ink, the corresponding CO_2 sensor was prepared by cutting a small square, *ca.* 5 mm, of the ink-coated Tyvek film and placing it between two 1 cm square layers of the 25 μm LDPE film. This sensor 'sandwich' was then heat-sealed using a heat press (VEVOR, London, UK) operated at 110 °C for 1 min. A wide range of such 'sandwich' LDPE/CO_2 sensors were prepared in this way using both the solvent- and water-based inks, each incorporating one of the following pH-sensitive dyes – cresol red (CR), *m*-cresol purple (MCP), α-naphtholphthalein (NP), xylenol blue (XB), thymol blue (TB), *o*-cresol purple (OCP) and thymolphthalein (TP). The chemical structures and key properties (pK_a value, absorption maxima of the protonated, HD, and deprotonated, D^-, forms) of these dyes are given in S2 in the ESI.† Each heat-sealed LDPE layer acts as a gas-permeable but ion-impermeable barrier which prevents interference from any non-gaseous, usually ionic, species in the growth medium. Photographs of a typical 1 cm square, heat-pressed (and so LDPE covered), CO_2 sensor are shown in S3 of Fig. S4 of the ESI,† showing a XB-silicone sensor in the presence and absence of CO_2, where its respective colour is blue and yellow.

The stability exhibited by these CO_2 sensors is demonstrated in Fig. S5 in the ESI,† which shows a plot of the unchanging measured apparent absorbance, A', of a XB-silicone sensor held in the LB growth medium at 30 °C over a period of 14 days. Other work showed that its sensitivity also remained unchanged over this period. Although volatile organics, such as methane, are not expected to be generated by the *E. coli* bacterium under test, other work showed that such a gas, which is not acidic nor very reactive, had no effect on the sensor's performance, see Fig. S6 in the ESI.†

2.3. Sensor placement and use in a typical CO_2 μR-TVC run

In all the bacterial studies reported here, the CO_2 sensor under test was placed at the bottom of a 15 mL conical (Falcon®) tube, to which was then added 9 mL of the sterile growth medium (LB broth), with an initial pH of 7. The run was initiated by adding 1 mL of an *E. coli* dispersion of known bacterial load (*e.g.*, 10^4 CFU mL^{-1}), at which point the Falcon® tube was sealed and placed in an incubator set at 30 °C, and the XB/silicone sensor then photographed as a function of incubation time, *t*, over a period of 16 h. A schematic illustration of a typical, inoculated, sealed Falcon® tube is illustrated in Fig. S7(a) in the ESI.† Usually, several different inoculations, covering the range 10^1 to 10^8 CFU mL^{-1} in tenfold steps, were prepared in this way and all the tubes loaded at the same time in the incubator and then photographed at regular hourly intervals as a function of *t*, see Fig. S7(b) in the ESI.†

As illustrated in Fig. S7(a),† the CO_2 sensor is placed with the sensor film facing the wall of the clear Falcon® tube so that it can be easily photographed and to prevent interference from any scattering or highly coloured species, which are obscured by the white Tyvek supporting substrate. The high gas permeability of the latter ensures the CO_2 sensor responds promptly to the any change in the $\%CO_2$ dissolved in the growth medium on the non-indicator side of the Tyvek.

2.4. Other methods

All photography was carried out using a Canon EOS 700D digital camera (Canon Inc., London, UK) with a D65 daylight lamp as the illumination source, and each recorded digital image of a colourimetric CO_2-sensitive sensor was processed for its red, green, and blue colour space values (*i.e.*, RGB values) using the freely available processing software, ImageJ,[18] from which a value for the apparent absorbance, A', of the sensor was derived.[19,20] When determining the sensitivity of the CO_2 sensors, α, the sensor was fixed in a glass gas cell and purged with the different CO_2 gas mixtures of known composition for 15 min, to ensure a full colour change was achieved, before the digital photograph of the sensor was taken.

3. Theory

Most colourimetric CO_2 sensors, including those used in this work, employ a pH indicator dye with protonated, HD, and deprotonated, D^-, forms that exhibit different colours. Thus, exposure to CO_2 causes a reversible colour change in the dried ink film due to the following equilibrium reaction,

$$D^- + CO_2 + H_2O \rightleftharpoons HD + HCO_3^- \quad (5)$$

Based on the above reaction, it can be shown that,

$$R = [HD]/[D^-] = (A_o - A)/(A - A_\infty) = \alpha \cdot x\%CO_2 \quad (6)$$

where R is the ratio of the concentration of HD and D^-, respectively, A_o and A_∞ are the absorbances of the sensor film in the absence (usually under Ar) and presence of a vast excess (usually 1 atm = 100% CO_2) of CO_2, respectively, and A is the absorbance of the film when the ambient CO_2 level is x%. As noted earlier, the parameter α (units: $\%CO_2^{-1}$) represents the sensitivity of the CO_2-sensor film, the inverse of which corresponds to the $\%CO_2$ at which the film is half-way through its colour change, when $[HD]/[D^-] = 1$.

In CO_2 μR-TVC, the threshold time, TT, is defined as the time at which the $\%CO_2$ reaches $1/\alpha$, the half-way colour change point. As in O_2 μR-TVC, the value of $\log(\text{CFU mL}^{-1})$ is found to be directly proportional to TT for a given inoculum.[21] Since α is primarily determined by the reciprocal of the dye's acid dissociation constant, K_a, CO_2 indicator films with a wide range of sensitivities can be made by using pH indicator dyes with varying pK_a values ($pK_a = -\log(K_a)$).

In a modified version of the kinetic bacterial growth model outlined earlier, it is assumed that the $\%CO_2$ generated at any time t mirrors the $\%O_2$ consumed, and is described by the simple expression, $\%CO_2 = 21 - \%O_2$. It follows that the model predicted variation in $\%CO_2$ generated as a function of incubation time is described by,

$$\%CO_2 = 21/[1 + A^*\exp(-t^*)] \quad (7)$$

Thus, eqn (7) was used to generate the plot of $\%CO_2$ *vs.* t^* illustrated in Fig. 2. From this data, the threshold time t^*_{TT} (at which point the $\%CO_2 = 1/\alpha$) was calculated for a range of α values, spanning 7 to 0.14% CO_2^{-1}, reflecting experimentally reasonable sensor sensitivities. The resulting α *vs.* t^* curve is also plotted in Fig. 2 as the broken red line.

A comparison of the model-predicted K_{sv} *vs.* t^*_{TT} and α *vs.* t^*_{TT} profiles in Fig. 1 and 2, respectively, for the O_2 μR-TVC and CO_2 μR-TVC systems, highlights a key advantage of the CO_2 μR-TVC approach. Specifically, by employing highly sensitive CO_2 indicators, the value of t^*_{TT} can be reduced well below the point at which $N(t)/N_{max} = 0.5$, $\%CO_2 = \%O_2 = 10.5\%$ and $t = t^*_{1/2}$. Crucially, this suggests that CO_2 μR-TVC, when implemented with high-sensitivity sensors, has the potential to achieve significantly faster TVC measurements than have been possible so far with conventional O_2 μR-TVC systems.

4. Results and discussion

The following two sections describe, respectively, how the sensitivity, α, of a typical CO_2 sensor was determined and how this sensor was then used to measure TT in a typical CO_2 μR-TVC experiment. In these sections, the example sensor employed was a solvent-based XB/silicone sensor; the α and TT values of all the other CO_2 sensors were then determined the same way.

4.1. Measurement of the sensitivity of a CO_2 sensor

The sensitivity of a typical CO_2 sensor, in this case a XB/silicone sensor, was measured at room temperature (20 °C) by recording its colour photographically in the presence of different $\%CO_2$/Ar mixtures of known composition, ranging from 0–100%, the results of which are illustrated in Fig. 3(a).

Previous work by this group has demonstrated that digital colour analysis (DCA) of a CO_2 colourimetric sensor can be used to generate apparent absorbance, A', values which are directly proportional to the actual absorbance, A. As such, A' can be used as a direct replacement for A in eqn (6) to calculate a R value for the $\%CO_2$ value under test, based on apparent (colour-based) values rather than actual (spectrophotometric-based) absorbance values.[19] In this work, for each $\%CO_2$ gas mixture tested, the red component, RGB (red), was extracted from the Red–Green–Blue (RGB)

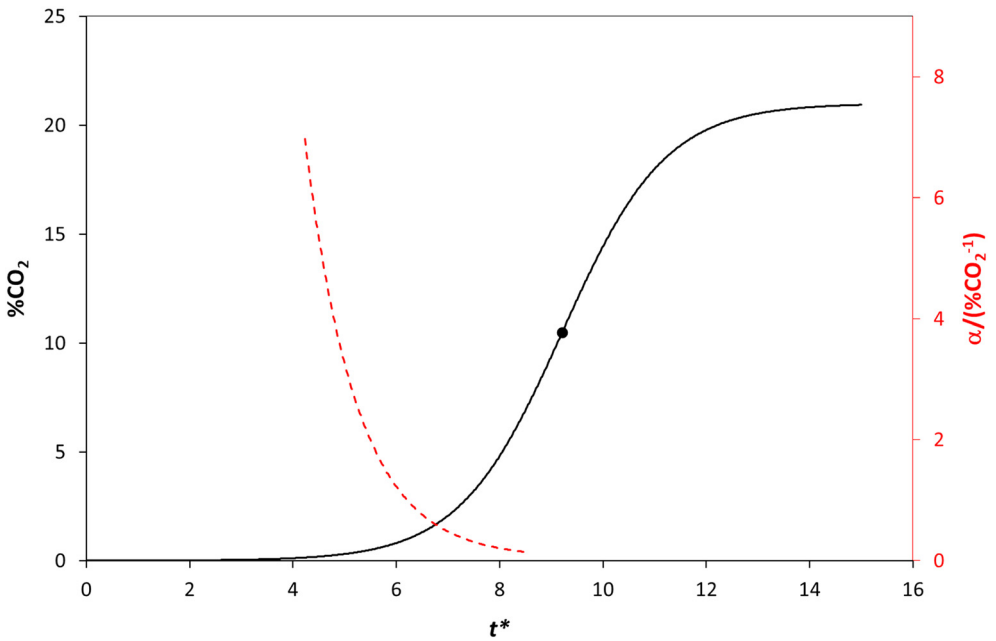

Fig. 2 Plot of $\%CO_2$ *vs.* unitless time parameter t^*, calculated using eqn (7), assuming N_{max} and N_o are 10^8 and 10^4 CFU mL^{-1}, respectively. The broken red line is a plot of the calculated variation in t^*_{TT} for a series of CO_2 sensors with different sensitivity, α, values spanning the range 0.14 to 7% CO_2^{-1}. The black point marks t^* value (9.2) when $N_o/N_{max} = 0.5$ and $\%CO_2 = \%O_2 = 10.5\%$.

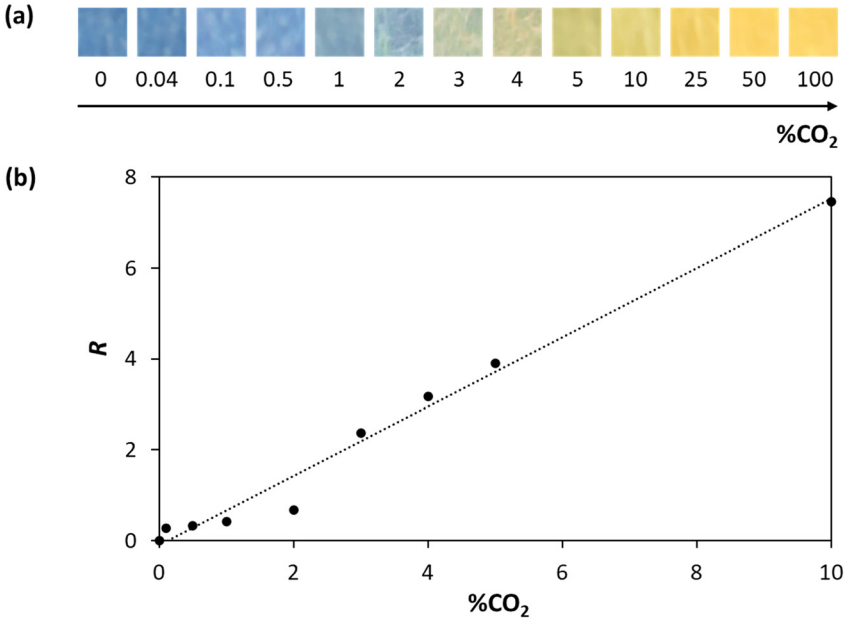

Fig. 3 (a) Photographs of the XB/silicone indicator in air at room temperature (20 °C), when exposed to different levels of $\%CO_2$ and (b) subsequent plot of the RGB-based data in (a) in the form of *R vs.* $\%CO_2$, where *R* was calculated using the apparent absorbance (*vide infra*), *A*′, values and eqn (6), and where the *A*′ values were determined *via* DCA of the photos in (a), with the A'_0 and A'_∞ values, 0.90 and 0.01, respectively, taken as the values of *A*′ in the absence and presence of 100% (1 atm) of CO_2, *vide infra*.

profile of the sensor's image. The corresponding value of *A*′ was then calculated using the following expression,

$$A' = \log(255/\mathrm{RGB(red)}) \quad (8)$$

The subsequent straight-line plot of *R vs.* $\%CO_2$ for the XB/silicone sensor, derived from the images in Fig. 3(a), is illustrated in Fig. 3(b). This yielded a sensitivity (or α) value of *ca.* 0.76% $\%CO_2^{-1}$, indicating a midway colour transition value (= $1/\alpha$) of *ca.* 1.3% CO_2.

The reproducibility and accuracy of a typical CO_2 sensor was tested using the same method as described in Fig. 3, using fixed mixture calibration gases, comprising, 0 (argon) and 0.1, 1, 5, 25 and 100% CO_2 in air, to evaluate ten XB/silicone sensors in terms of their respective, A'_0, A_∞ and α values. The results of this work are illustrated in Fig. S8 in the ESI† and reveal little variation in all three of these key parameters, with α = 0.74 ± 0.04 (5.4%) $\%CO_2^{-1}$. All the CO_2 sensors tested exhibited similar, small variances in these parameters, indicating the sensors have a good degree of accuracy and reproducibility for measuring CO_2.

Finally, the 90% response time, $t(90)_\downarrow$, and recovery time, $t(90)_\uparrow$, of the XB/silicone CO_2 sensor at 20 °C were determined by monitoring *A*′ as the sensor was cycled between air and 5% CO_2. The results of this work are illustrated in Fig. S9 in the ESI,† from which $t(90)_\downarrow$ and $t(90)_\uparrow$ values of 2.8 and 7.1 min were calculated, respectively. These values are typical of all the CO_2 sensors tested, and appropriate for use in $\%CO_2$ μR-TVC, since the colour transition due to the exponential growth phase typically occurs over 1–2 h.

4.2. Measurement of TT in a typical μR-TVC run using a CO_2 sensor

The same protocol as used in O_2 μR-TVC for measuring the TT in a typical micro-respirometry run was employed in this CO_2 μR-TVC study, using the CO_2 sensors described in section 2.2.[5] In a typical experiment, an inoculum of 10^4 CFU mL^{-1} *E. coli* was added to the Falcon® tube containing the XB/silicone sensor, which was then photographed as a function of incubation time, *t*. A selection of these photographic images is shown in Fig. 4(a), illustrating the colour change of the initially blue indicator to yellow over time as bacterial growth produced increasing amounts of CO_2. DCA of these images, based on eqn (8), was used to generate the apparent absorbance, *A*′, *vs. t* data plotted in Fig. 4(b). As expected, the plot exhibits initially little change in colour (the incubation period), followed by a period of rapid colour change as the initial bacterial load in the Falcon® tube grew exponentially.

Although it is possible to calculate the dissolved level of $\%CO_2$ in the growth medium at any time *t* from the calculated value of *A*′ using eqn (6), this is an additional and unnecessary step, just as it is unnecessary to calculate the $\%O_2$ from the recorded lifetime values in O_2 μR-TVC. Instead, in CO_2 μR-TVC, the value of TT is taken as the midpoint of the sensor's colour change, *i.e.*, when $A' = (A'_0 + A'_\infty)/2$. This point is indicated by the broken red lines in Fig. 4(b). As will

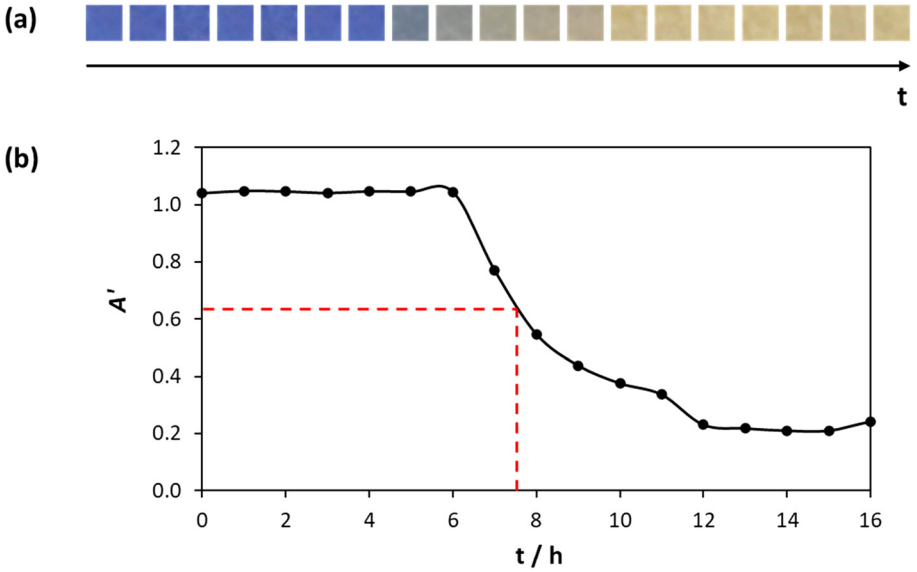

Fig. 4 (a) Photographs of the XB/silicone indicator in a typical CO_2 μR-TVC experiment using a 10^4 CFU mL^{-1} inoculum of *E. coli* and (b) plot of the results of DCA analysis of the images in (a) in the form of A' *vs.* t. The red, broken horizontal and vertical lines highlight the time point (TT) when the sensor is half-way through its colour change.

be shown later, repeating this experiment across a range of known bacterial loads yields a linear calibration curve of log(CFU mL^{-1}) *vs.* TT, which can then be used to determine the TVC of unknown samples. As noted earlier, all microbiological assays were carried out in triplicate and the average value taken. In all cases, the standard deviation was ≤10%, which is significantly lower than that typically reported for the APC method (18% for counts above 30).[22,23] Previous work using 3D-printed CO_2 sensors has demonstrated that CO_2 μR-TVC is statistically equivalent to O_2 μR-TVC,[21] which itself has been shown to be equivalent to the gold-standard APC method.[24]

The repeatability of the CO_2 sensors in CO_2 μR-TVC was tested by making ten XB/silicone sensors and running the same micro-respirometry experiment as outlined above, see Fig. 4. The results, illustrated in Fig. S10 in the ESI,† show a series of near superimposable A' *vs.* t curves, with an average TT of 7.9 ± 0.2 h (*ca.* 2.5%). This variance is comparable to that reported for 3D-printed CO_2 sensors (2.4%) and commercial O_2 sensors (3.0%) in μR-TVC applications.[21,24]

Sensor durability and stability were also assessed by testing the performance of a single XB/silicone sensor held in the same (un-inoculated) growth medium on five consecutive days at 30 °C. As shown in Fig. S11 in the ESI,† the values of A'_0, A'_∞ and α remain unchanged over five consecutive days, indicating no loss in sensitivity. These findings are consistent with the results presented in Fig. S5,† which showed stable A'_0 values over a 14-day period.

4.3. The relationship between TT and CO_2 sensor sensitivity, α

All CO_2 indicators prepared in this work were initially characterised and tested as described in sections 4.1 and 4.2. These analyses yielded values for sensitivity (α) and threshold time (TT) using an initial *E. coli* load of 10^4 CFU mL^{-1}, and the corresponding colour change profiles over time are given in Table 1. Although most of the CO_2 sensors tested produced striking colour changes, the phthalein dye-based sensors (OCP and TP*) exhibited paler colours post heat-sealing, appearing somewhat washed out. Additionally, these phthalein-based indicators showed reduced stability compared to the others and required 1–2 mL of extra base to be added to the standard ink formulation to produce effective sensors, see Table 1. Despite these limitations, the phthalein indicators were still usable. Notably, the TP*-based sensor was found to be the most sensitive of all CO_2 sensors tested, and thus potentially the fastest for total viable count (TVC) measurements. However, its poor stability remains a significant barrier to routine application.

As predicted by the kinetic model (see Fig. 2), for a fixed bacterial load, such as 10^4 CFU mL^{-1} used in this work, TT should decrease with increasing CO_2 sensor sensitivity. This trend is supported by the plot of the data in Table 1 in the form of TT *vs.* α, illustrated in Fig. 5, which shows a clear linear relationship with a negative gradient. A *t*-test analysis comparing the slopes of the TT *vs.* α regression lines for the solvent- and water-based sensors found no statistically significant difference between them ($P = 0.46$).

The plot shows that, as predicted by the kinetic model, the value of TT can be markedly reduced by increasing the sensitivity (α) of the CO_2 sensor, thereby allowing much faster TVC measurements in CO_2 μR-TVC. This is in direct contrast to O_2 μR-TVC, where both model (Fig. 1) and experimental data[5] show that TT increases with O_2 sensor sensitivity (K_{SV}) and is always greater than $t^*_{1/2}$. The results in Fig. 5 suggest that using a very sensitive CO_2 sensor

Table 1 Summary of results for the CO_2 sensors when assessed for sensitivity and TT value

Dye	pK_a	α (%CO_2^{-1})	TT (h)	Hourly photographic images of the sensor when inoculated with 10^4 *E. coli*
Solvent-based indicators				
CR	8.2	0.09	9.0	
MCP	8.3	0.22	7.9	
NP	8.5	0.66	7.6	
XB	8.9	0.76	7.5	
TB	8.9	0.98	6.9	
TB†	8.9	1.16	6.0	
Water-based indicators				
CR	8.2	0.02	9.0	
MCP	8.3	0.06	8.9	
NP	8.5	0.19	8.8	
XB	8.9	0.41	8.5	
TB	8.9	0.48	7.7	
OCP[b]	9.4	0.90	6.8	
TP*[a]	10.0	1.91	4.1	

[a] An extra 1 mL of base was added to standard ink formulation. [b] An extra 2 mL of base was added to standard ink formulation. Photographs recorded every 30 minutes for TP* indicator. TB† refers to the TB/Ethyl cellulose (EC)/TOAH ink-based sensor.[16]

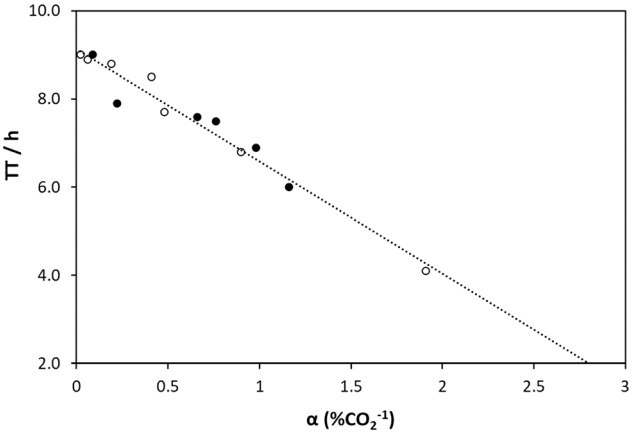

Fig. 5 Plot of TT *vs.* CO_2 sensor sensitivity (α) using data taken from Table 1. The open and closed circles refer to water and solvent based CO_2 sensors, respectively. The gradient and intercept of the line of best fit to all the data are −2.54 ± 0.16 and 9.13 ± 0.12, respectively.

could enable TVC to be measured much faster (possibly in minutes rather than hours) than is currently possible with conventional O_2 μR-TVC, which itself is much faster than the standard APC method. This is very promising since CO_2 μR-TVC, like O_2 μR-TVC, is amenable to automation and so capable of measuring the TVC of many samples at the same time. Finally, the *x*-intercept value of the line of best fit to the data in Fig. 5 suggests that a sensor with an α value ≥3.6% CO_2^{-1} would be capable of detecting CO_2 production during the lag phase of bacterial growth, when the bacteria are respiring but not yet multiplying rapidly.

For simplicity, the kinetic model described in section 3 assumes that all the CO_2 generated by the bacteria appears as dissolved CO_2 in the growth medium, which, in practice is unlikely. However, the model also shows that the shape of the profile would be identical to that predicted by the model (see Fig. 2) if the pH of the growth medium remained constant during a run, as might be achieved using a pH buffer. For example, if the pH of the growth medium stayed at pH 7 through a kinetic run, although only 18% of the model predicted %CO_2 would appear as dissolved CO_2, the shape of the actual %CO_2 *vs. t* run would be the same as that illustrated in Fig. 2, but with all the model predicted %CO_2 values multiplied by 0.18.

In this work, no additional pH buffer was added, and the pH was found to remain at pH 7 for *ca.* 6 h before dropping to pH 6 after 10 h, as illustrated in Fig. S12 in the ESI.† The effects of this pH change on the model-predicted %CO_2 *vs.* t^* and α *vs.* t^*_{TT} curves are illustrated in Fig. S13 in the ESI,† and show that, despite this change in pH, the shapes of both curves remain similar to those illustrated in Fig. 2. Also unchanged is the key predicted feature of the model, namely that increasing sensor sensitivity reduces TT, thereby enabling faster analysis, as established experimentally by the TT *vs.* α plot illustrated in Fig. 5.

As noted earlier, this plot suggests a sensor with a sensitivity ≥3.6% CO_2^{-1} would be ideal for rapid CO_2 μR-TVC measurements. However, given the ambient level of CO_2 in air is *ca.* 0.04%, it is likely that sensors with $\alpha \geq 25\%$ CO_2^{-1} would likely be too sensitive for practical use in CO_2 μR-TVC. For this reason, model predicted variations of α *vs.* t^*_{TT} were limited to the experimentally realistic range of 0.14 to 7.0% CO_2^{-1}.

4.4. Examples CO_2 μR-TVC calibration plots

To demonstrate the efficacy of CO_2 μR-TVC for determining total viable count of a sample with an unknown bacterial load of *E. coli*, two distinct CO_2-sensitive sensors, namely a solvent-based one, XB/silicone, and a water-based one, TP*/HPC, were prepared and used as described in section 4.2. *A′ vs. t* plots were generated for a series of *E. coli* inocula of known bacterial loads, spanning from 10^1 to 10^8 CFU mL^{-1}, incubated at 30 °C. For each inoculum, the sensor's colour change was monitored photographically as a function of time. Digital colour analysis (DCA) of the resulting images produced *A′ vs. t* plots, from which the threshold time (TT) was extracted, and used to construct calibration plots of log(CFU mL^{-1}) *vs.* TT for each sensor. The results of this work, comprising of (a) the photographic images of the CO_2 indicator as a function of *t* for the different bacterial loads, (b) the corresponding *A′ vs. t* plots, and (c) the log(CFU mL^{-1}) *vs.* TT calibration curves for the XB/silicone (α = 0.76% CO_2^{-1}) and TP*/HPC (α = 1.91% CO_2^{-1}) sensors are illustrated in Fig. 6 and 7, respectively.

As seen in Fig. 6(b) and 7(b), both CO_2 sensors give linear log(CFU mL^{-1}) *vs.* TT calibration plots, which can then be used to determine the TVC of unknown samples of *E. coli*. The gradients of the lines of best fit in the calibration curves, Fig. 6(c) and 7(c), are −0.64 and −1.09 log(CFU mL^{-1}) h^{-1}, respectively, demonstrating that the more sensitive TP*/HPC sensor enables TVC measurements to be conducted approximately 70% faster than the XB/silicone sensor. For comparison, the same experiment conducted using an O_2 sensor yields a gradient of −0.74 log(CFU mL^{-1}) h^{-1}, which is like that of the XB/silicone CO_2 sensor, but, as expected, much lower (and so slower) than the TP*/HPC sensor. However, as noted earlier, the TP*/HPC sensor exhibits poor stability in growth media, for reasons that are unclear at present. This is made apparent from the near superimposable *A′ vs. t* plots illustrated in Fig. 7(b) for the 10^3–10^1 and control (no bacteria) runs, and the vertical drop in the otherwise straight-line trend observed in the log(CFU mL^{-1}) *vs.* TT plot in Fig. 7(c). Thus, although this work shows that it is possible to create a very rapid method for the measurement of the TVC of aerobes (or anaerobes for that matter) based on CO_2 μR-TVC using a highly sensitive CO_2 sensor, the most sensitive CO_2 sensors currently available, such as the TP*/HPC sensor, lack stability for their routine use. Encouragingly, all other CO_2

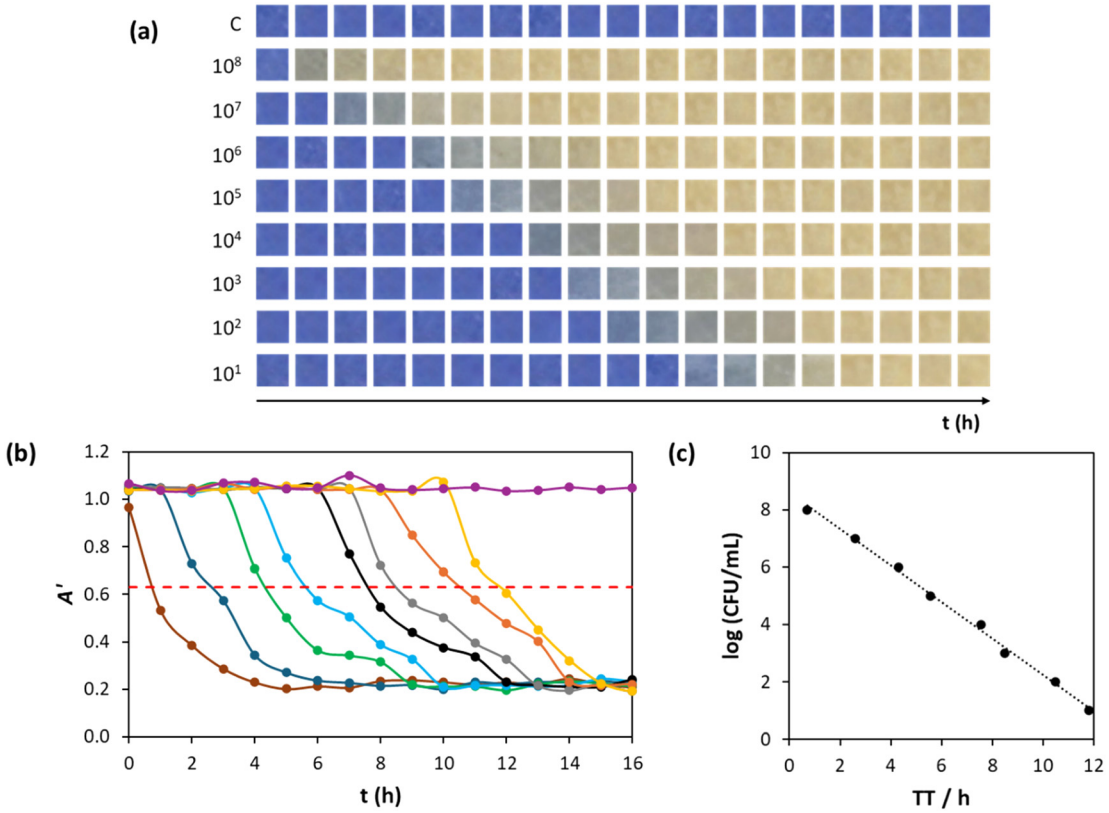

Fig. 6 (a) Photographic images of the XB/silicone indicator in a CO_2 μR-TVC study, in which the bacterial load of *E. coli* was varied over the range 10^8 to 10^1 CFU mL^{-1}, (b) plots of *A′ vs. t* for each different inoculum, calculated using DCA analysis of the images in (a) and eqn (8) (the red broken line highlights the mid colour-change point which was used to derive values for TT for each inoculum), (c) plot of the log(CFU mL^{-1}) *vs.* TT data derived from (b).

sensors tested in this work were found to be stable in growth medium for several weeks, suggesting that with further work, a stable, highly sensitive alternative to TP*/HPC may be developed for reliable, rapid TVC measurements.

5. Conclusions

The measurement of total viable count (TVC) using oxygen-based micro-respirometry, O_2 μR-TVC, is an established, commercial method which is faster, usually <24 h, than the more traditional aerobic plate counting (APC) method, typically <72 h.[4] However, both kinetic modelling and experimental observations[5] show that the speed of O_2 μR-TVC is largely limited by the time taken to significantly deplete the dissolved $\%O_2$ in growth medium, $t^*_{1/2}$, which occurs only when the bacterial concentration has grown to a significant level, typically, $N_{max}/2$.

In contrast, the new CO_2-based micro-respirometry method described here, CO_2 μR-TVC, does not require the bacterial load to reach such high levels and so can be used to make much faster TVC measurements. This work demonstrates a clear, direct inverse relationship between TT and the sensitivity of the CO_2 sensor, α, and that very short analysis times (<1 h) should be possible using very sensitive ($\alpha \geq 3.3\%$ CO_2^{-1}) CO_2 sensors. However, to realise the very rapid measurement potential of CO_2 μR-TVC, a stable, high sensitivity CO_2 sensor needs to be developed, and work is currently in progress to achieve this goal.

The advantages of CO_2 μR-TVC over the traditional APC method include all those associated with O_2 μR-TVC, namely a simple, non-subjective, low-cost method for measuring TVC, which is amenable for automation and so the simultaneous, rapid analysis of many samples. Unlike APC, it does not require the use of a large amount of plasticware, nor significant technical support, and does not have a subjective element. APC has a subjective element in that the plate number returned is a skilled technician's interpretation of the number of colonies on the plate, which often varies from technician to technician and laboratory to laboratory.[25] Furthermore, CO_2 μR-TVC has been shown to be statistically equivalent to O_2 μR-TVC,[21] which in turn is equivalent to APC.[24] Most importantly, CO_2 μR-TVC is capable of much faster analysis times than O_2 μR-TVC, which in turn are much faster than APC. Consequently, once an appropriate, high sensitivity CO_2 sensor has been developed, it is likely commercial CO_2 μR-TVC instrumentation will emerge that will make CO_2 μR-TVC the go to alternative to the APC

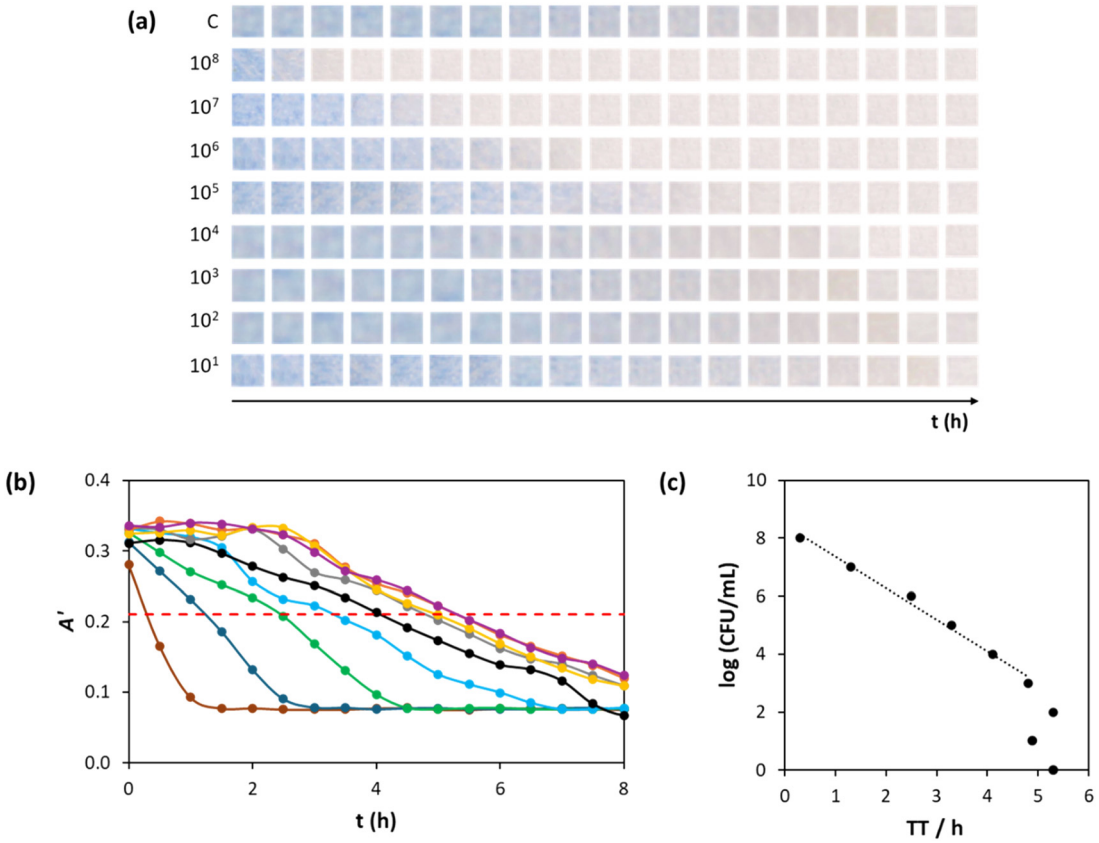

Fig. 7 As in Fig. 6, (a) photographic images of the TP*/HPC indicator in a CO_2 μR-TVC study, in which the bacterial load of *E. coli* was varied over the range 10^8 to 10^1 CFU mL^{-1}, (b) plots of *A′ vs. t* for each different inoculum, calculated using DCA analysis of the images in (a) and eqn (8) (the red broken line highlights the mid colour-change point which was used to derive values for TT for each inoculum), (c) plot of the log(CFU mL^{-1}) *vs.* TT data derived from (b).

method that is currently employed in most microbiology laboratories.

Data availability

The data supporting the findings of this work are available within the article. Source data underlying the graphs presented in the main figures are included in the ESI.†

Author contributions

Sean Cross: validation, formal analysis, investigation, writing – original draft. Christopher O'Rourke: methodology, supervision and visualization. Andrew Mills: conceptualization, writing – review & editing, supervision, project administration, funding acquisition.

Conflicts of interest

There are no conflicts of interests to declare.

Acknowledgements

This work was funded by the EPSRC (EP/T007575/1).

References

1 S. Elisseeva, E. Santovito, E. Linehan, J. P. Kerry and D. B. Papkovsky, *Sens. Actuators, B*, 2023, **383**, 133582.
2 Y. Tanaka, H. Takahashi, A. Imai, T. Asao, S. Kozaki, S. Igimi and B. Kimura, *Food Control*, 2010, **21**, 1075–1079.
3 V. Jasson, L. Jacxsens, P. Luning, A. Rajkovic and M. Uyttendaele, *Food Microbiol.*, 2010, **27**, 710–730.
4 A. Hempel, N. Borchert, H. Walsh, K. R. Choudhury, J. P. Kerry and D. B. Papkovsky, *J. Food Prot.*, 2011, **74**, 776–782.
5 S. Cross, D. Yusufu, C. O'Rourke and A. Mills, *Chemosensors*, 2024, **12**, 190.
6 Oculer, **https://www.oculer.com/**, (accessed May 2025).
7 M. G. Corradini and M. Peleg, *J. Appl. Microbiol.*, 2005, **99**, 187–200.
8 D. B. Papkovsky and J. P. Kerry, *Sensors*, 2023, **23**, 4519.
9 X. Luo, A. Zaitoon and L. T. Lim, *Compr. Rev. Food Sci. Food Saf.*, 2022, **21**, 2489–2519.
10 W. Heo and S. Lim, *Foods*, 2024, **13**, 3047.
11 G. T. Huynh, V. Kesarwani, J. A. Walker, J. E. Frith, L. Meagher and S. R. Corrie, *Front. Chem.*, 2021, **9**, 728717.
12 Y. Zhang, H. Yang, W. Gao and C. Wu, *IEEE Sens. J.*, 2024, **24**, 29564–29574.

13 E. Santovito, S. Elisseeva, J. P. Kerry and D. B. Papkovsky, *Sens. Actuators, B*, 2023, **390**, 134016.
14 ISO 18593, 2018, *International Organization for Standardization*, Geneva, Switzerland, 2018.
15 ISO 4833-1, 2013, *International Organization for Standardization*, Geneva, Switzerland, 2013.
16 A. Mills and Q. Chang, *Sens. Actuators, B*, 1994, **21**, 83–89.
17 Karkimya, **https://www.karkimya.com.tr/en/products/film-application/k-hand-coater-k-bar**, (accessed May 2025).
18 ImageJ, **https://imagej.net/ij/index.html**, (accessed May 2025).
19 D. Yusufu and A. Mills, *Sens. Actuators, B*, 2018, **273**, 1187–1194.
20 L. McDonnell, D. Yusufu, C. O'Rourke and A. Mills, *Chemosensors*, 2022, **10**, 544.
21 L. McDonnell, D. Yusufu and A. Mills, *Analyst*, 2024, **149**, 5582–5590.
22 R. Eden, Enterobacteriaceae, coliforms and *E. coli* – classical and modern methods for detection and enumeration, in *Encyclopedia of Food Microbiology*, ed. C. A. Batt and M. L. Tortorello, Academic Press, Cambridge, MA, USA, 2nd edn, 2014, pp. 667–673.
23 M. L. J. Weitzel, C. S. Vegge, M. Pane, V. S. Goldman, B. Koshy, C. H. Porsby, P. Burguière and J. L. Schoeni, *Front. Microbiol.*, 2021, **12**, 693066.
24 E. Santovito, S. Elisseeva, A. Bukulin, J. P. Kerry and D. B. Papkovsky, *Biosens. Bioelectron.*, 2021, **176**, 112938.
25 S. Sutton, *J. Valid. Technol.*, 2011, **17**, 42–46.